Please note that Cypress is an Infineon Technologies Company.
The document following this cover page is marked as “Cypress” document as this is the company that originally developed the product. Please note that Infineon will continue to offer the product to new and existing customers as part of the Infineon product portfolio.

Continuity of document content
The fact that Infineon offers the following product as part of the Infineon product portfolio does not lead to any changes to this document. Future revisions will occur when appropriate, and any changes will be set out on the document history page.

Continuity of ordering part numbers
Infineon continues to support existing part numbers. Please continue to use the ordering part numbers listed in the datasheet for ordering.

THIS SPEC IS OBSOLETE

Spec No: 002-05408

Spec Title: AN205408 - SMO BASED FIELD ORIENTED CONTROL OF INDUCTION MOTOR WITH SPEED SENSOR

Replaced by: NONE

AN205408

SMO Based Field Oriented Control Of Induction Motor With Speed Sensor

Associated Part Family: MB9AXXX/MB9BXXX Series

This document describes three-phase squirrel-cage induction motor drive by sensor-FOC scheme, which applies sliding mode algorithm for rotor flux estimation.

Contents

1 Introduction

1.1 Purpose

This document describes three-phase squirrel-cage induction motor drive by sensor-FOC scheme, which applies sliding mode algorithm for rotor flux estimation.

1.2 Definitions, Acronyms and Abbreviations

- FOC: Field Oriented Control
- PID: Proportion, Integration, Derivation Regulator
- SMO: Sliding Mode Observer
- SVPWM: Space Vector Pulse Width Modulation
- DOF: Degree of Freedom
- RLS: Recursive Least Square
- $V_{\alpha s}$: Stator voltage in α-axis
- $V_{\beta s}$: Stator voltage in β-axis
- $i_{\alpha s}$: Stator current in α-axis
- $i_{\beta s}$: Stator current in β-axis
- $\lambda_{\alpha s}$: Stator flux linkage in α-axis
- $\lambda_{\beta s}$: Stator flux linkage in β-axis
- $V_{\alpha r}$: Rotor voltage in α-axis
- $V_{\beta r}$: Rotor voltage in β-axis
- $i_{\alpha r}$: Rotor current in α-axis
- $i_{\beta r}$: Rotor current in β-axis

- $\lambda_{\alpha r}$: Rotor flux linkage in α-axis
- $\lambda_{\beta r}$: Rotor flux linkage in β-axis
- V_{ds}: Stator voltage in d-axis
- V_{qs}: Stator voltage in q-axis
- i_{ds}: Stator current in d-axis
- i_{qs}: Stator current in q-axis
- λ_{ds}: Stator flux linkage in d-axis
- λ_{qs}: Stator flux linkage in q-axis
- V_{dr}: Rotor voltage in d-axis
- V_{qr}: Rotor voltage in q-axis
- i_{dr}: Rotor current in d-axis
- i_{qr}: Rotor current in q-axis
- λ_{dr}: Rotor flux linkage in d-axis
- λ_{qr}: Rotor flux linkage in q-axis
- R_s: Stator resistance
- R_r: Rotor resistance
- L_m: Mutual inductance
- L_{ls}: Stator leakage inductance
- L_{lr}: Rotor leakage inductance
- $L_s = L_m + L_{ls}$: Stator self-inductance
- $L_r = L_m + L_{lr}$: Rotor self-inductance
- θ_Ψ: Rotor flux angle
- ω_r: Rotor speed (electrical)
- ω: Synchronous speed
- T_e: Electrical torque of motor
- V_{qlim}: Maximum available voltage of V_{qs}
- V_{dlim}: Maximum available voltage of V_{ds}

1.3 Document Overview

The rest of document is organized as the following:

Chapter 2 describes off-line parameter measurement method.

Chapter 3 explains the realization of FOC scheme.

Chapter 4 shows the experiment result of the design control system.

2 Off-Line Parameter Measurement

In this chapter, off-line motor parameter measurement is introduced.

2.1 Overview

In the field oriented control, induction motor parameters are necessary since the flux observer is founded by motor model. For widely application and adaption of this scheme, parameter measurement becomes crucial before driving motor.

This chapter introduces an off-line parameter measurement method, which measures motor parameter through DC test, lock-rotor test and no load test. Although off-line parameter measurement cannot be precise enough, it is possible to implement FOC algorithm and then add on-line parameter identification to realize accurate driving for unknown induction motor.

2.2 Off-line Parameter Measurement

2.2.1 Equivalent Circuit of Induction Motor

Figure 1. Equivalent circuit of an induction motor

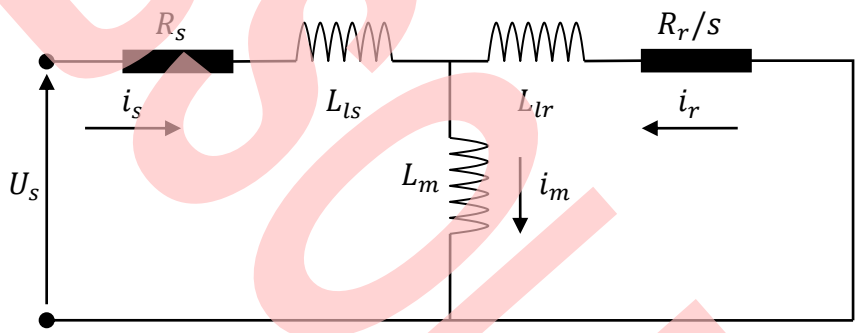

Figure 1. Equivalent circuit of an induction motor shows the equivalent circuit of an induction motor in steady state with balanced three-phase input. To measure motor parameters, three steady states are established, which are DC test, lock-rotor test, and no-load test.

2.2.2 DC Test

In the DC test, a DC voltage is imposed on stator, thus the inductances (L_{ls}, L_{lr}, and L_m) are regarded to be shorted. In another hand, rotor current i_r becomes zero and the equivalent circuit is simplified as Figure 2 therefore, stator resistance R_s is measured. In this application, a recursive least square (RLS) filter is applied to extract resistance information from imposed voltage and measured current.

Figure 2. Equivalent circuit under DC test

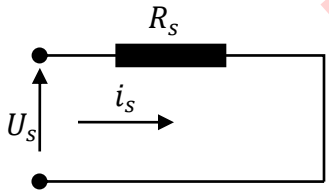

2.2.3 Lock-Rotor Test

In motor manufacturing, the lock-rotor test is usually done by block rotor with special tools, and then a balanced three-phase AC voltage is injected.

Figure 3 shows the equivalent circuit of an induction motor under lock-rotor test. The equivalent impendence at rotor side becomes R_r because the slip rate (s) equals to 1. In this case, the paralleled two impedances is assumed that $R_r + j\omega L_{lr} \ll j\omega L_m$.

Figure 3. Equivalent circuit under Lock-rotor test

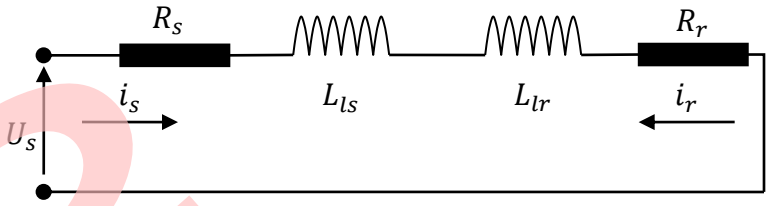

In practice, the rotor is difficult to lock without special tool, thus another conduction mode is introduced as Figure 4 shows. It is easy to prove that in this conduction mode, the phase equivalent circuit is same as Figure 3

Figure 4. Conduction pattern for lock-rotor test

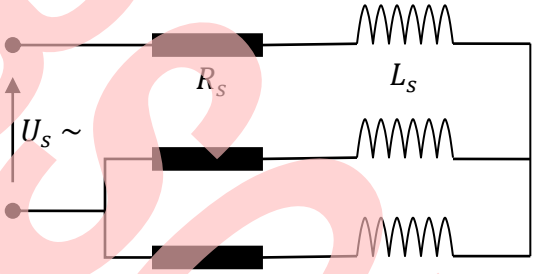

Now assuming $L_{ls} = L_{lr}$, when R_s is known, the equivalent impendence can be measured through input power, voltage, and current, and R_r and L_{ls} can be calculated sequentially.

2.2.4 No-Load Test

In no-load case, the rotor speed is assumed be equal to synchronous speed, and slip rate $s = 0$ is obviously obtained. Thus right hand part of the equivalent circuit in Figure 5 is an open circuit and was simplified as Figure 5 Therefore, the stator self-inductance $L_s = L_m + L_{ls}$ can be measured.

Figure 5. Equivalent circuit under no-load test

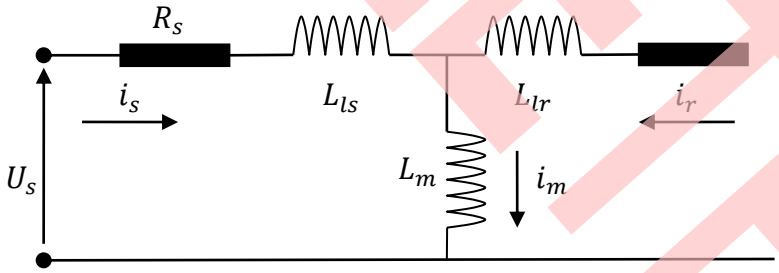

3 FOC Drive of Induction Motor

This chapter introduces induction motor model, principle of FOC drive, and the realization algorithm of FOC drive.

3.1 Rotor Flux Field Oriented Control

3.1.1 Mathematic Model of Induction Motor

Figure 6. Reference frame for motor modeling

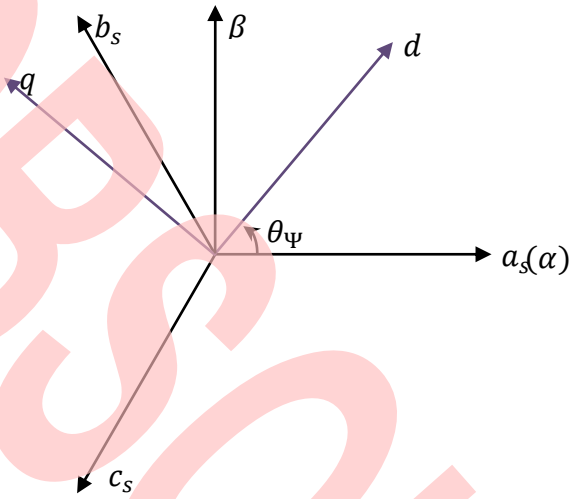

Same as most of electric rotating machine, a three-phase induction motor can be modeled in stationary $\alpha\beta$ reference frame and synchronous rotating dq reference frame.

Applying Clark transformation to three-phase squirrel cage induction motor model, motor dynamics in $\alpha\beta$ reference frame is described as below

$$V_{\alpha s} = R_s i_{\alpha s} + \frac{d}{dt}\lambda_{\alpha s} \quad \textbf{(3.1)}$$

$$V_{\beta s} = R_s i_{\beta s} + \frac{d}{dt}\lambda_{\beta s} \quad \textbf{(3.2)}$$

$$0 = V_{\alpha r} = R_r i_{\alpha r} + \frac{d}{dt}\lambda_{\alpha r} + \omega_r \lambda_{\beta r} \quad \textbf{(3.3)}$$

$$0 = V_{\beta r} = R_r i_{\beta r} + \frac{d}{dt}\lambda_{\beta r} - \omega_r \lambda_{\alpha r} \quad \textbf{(3.4)}$$

where the flux linkages has the following relationship with current

$$\lambda_{\alpha s} = L_{ls} i_{\alpha s} + L_M (i_{\alpha s} + i_{\alpha r}) = L_s i_{\alpha s} + L_M i_{\alpha r} \quad \textbf{(3.5)}$$

$$\lambda_{\beta s} = L_{ls} i_{\beta s} + L_M (i_{\beta s} + i_{\beta r}) = L_s i_{\beta s} + L_M i_{\beta r} \quad \textbf{(3.6)}$$

$$\lambda_{\alpha r} = L_{lr} i_{\alpha r} + L_M (i_{\alpha s} + i_{\alpha r}) = L_M i_{\alpha s} + L_r i_{\alpha r} \quad \textbf{(3.7)}$$

$$\lambda_{\beta r} = L_{lr} i_{\beta r} + L_M (i_{\beta s} + i_{\beta r}) = L_M i_{\beta s} + L_r i_{\beta r} \quad \textbf{(3.8)}$$

Taking Park transformation to above equations, induction motor model in dq reference frame is

$$V_{ds} = R_s i_{ds} + \frac{d}{dt}\lambda_{ds} - \omega \lambda_{qs} \quad \textbf{(3.9)}$$

$$V_{qs} = R_s i_{qs} + \frac{d}{dt}\lambda_{qs} + \omega\lambda_{ds} \quad \textbf{(3.10)}$$

$$0 = V_{dr} = R_r i_{dr} + \frac{d}{dt}\lambda_{dr} - (\omega - \omega_r)\lambda_{qr} \quad \textbf{(3.11)}$$

$$0 = V_{qr} = R_r i_{qr} + \frac{d}{dt}\lambda_{qr} + (\omega - \omega_r)\lambda_{dr} \quad \textbf{(3.12)}$$

$$\lambda_{ds} = L_{ls} i_{ds} + L_M(i_{ds} + i_{dr}) = L_s i_{ds} + L_M i_{dr} \quad \textbf{(3.13)}$$

$$\lambda_{qs} = L_{ls} i_{qs} + L_M(i_{qs} + i_{qr}) = L_s i_{qs} + L_M i_{qr} \quad \textbf{(3.14)}$$

$$\lambda_{dr} = L_{lr} i_{dr} + L_M(i_{ds} + i_{dr}) = L_M i_{ds} + L_r i_{dr} \quad \textbf{(3.15)}$$

$$\lambda_{qr} = L_{lr} i_{qr} + L_M(i_{qs} + i_{qr}) = L_M i_{qs} + L_r i_{qr} \quad \textbf{(3.16)}$$

The electric torque of induction motor can be expressed by the cross product of flux vector and current vector that

$$T_e = \frac{3}{2}P(\lambda_{ds} i_{qs} - \lambda_{qs} i_{ds}) = \frac{3}{2}P(\lambda_{qr} i_{dr} - \lambda_{dr} i_{qr}) \quad \textbf{(3.17)}$$

3.1.2 Rotor Flux FOC Principle

There are kinds of FOC schemes for induction motor drive, such as rotor flux FOC, stator flux FOC, and air gap flux FOC. In this document, rotor flux FOC is introduced.

From equation (3.17), it can be found that the electric torque is maximized for a given magnitude of rotor flux if set the current vector perpendicular to the flux vector, and this is how rotor flux FOC works.

Let's set the flux vector and current vector as below

$$[\lambda_{dr}, \lambda_{qr}] = [constant, 0] \quad \textbf{(3.18)}$$

$$[i_{dr}, i_{qr}] = [0, i_{qr}] \quad \textbf{(3.19)}$$

It is apparent that equations (3.18) and (3.19) define two perpendicular vectors such as rotor flux FOC requires. Substitute above two equations into motor model, the magnitudes of rotor flux vector and current vector are

$$\lambda_{dr} = L_M i_{ds} \quad \textbf{(3.20)}$$

$$i_{qr} = -\frac{L_M}{L_r} i_{qs} \quad \textbf{(3.21)}$$

$$T_e = -\frac{3}{2}P\lambda_{dr} i_{qr} = \frac{3}{2}P\frac{L_M^2}{L_r} i_{ds} i_{qs} \quad \textbf{(3.22)}$$

Above equations show that if (3.18) and (3.19) satisfy, rotor flux level is set solely by i_{ds}, and electric torque is controlled by i_{qs}. Thus, rotor flux vector and electric torque are controlled by i_{ds} and i_{qs} independently.

Based on aforementioned knowledge, the rotor flux field oriented control is established. Depicts the control structure of a sensor based rotor FOC driving, in which sliding mode observer is applied to estimate rotor flux vector.

Figure 7. Induction motor sensor-FOC control scheme

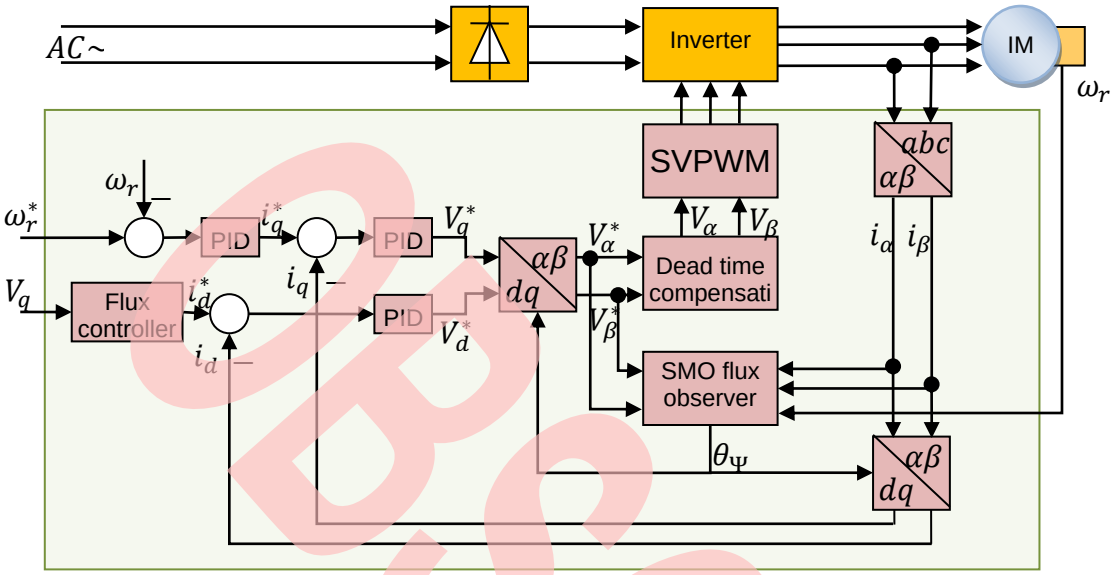

In the demo system, the sensor-FOC scheme mainly contains three modules. The control module is designed in dq reference frame that drives i_{ds} to a constant to assure constant rotor flux linkage, and the reference torque current i_{qs}^* is generated by speed regulator thus speed is tracked.

Another important module is SMO flux observer, which is designed in $\alpha\beta$ reference frame to estimate rotor flux vector, including its magnitude and position angle.

The dead time compensation algorithm and SVPWM is implemented to realize command voltage. And finally sensor based feedback FOC control system is constructed.

3.2 FOC Algorithm Realization

3.2.1 Back Calculation and Tracking PID regulator

The PID regulator is widely applied in most of control occasions, and its transfer function is

$$u(s) = K_p(1 + K_i\frac{1}{s} + \frac{1}{K_d}s)e(s) \quad \textbf{(3.23)}$$

Equation (3.23) shows a 1-DOF PID regulator, and it suffers reference kick and response kick due to direct proportion term and derivative term. In another hand, once the PID parameters are tuned, its performance on handling noise is also inherent. To overcome above shortages, a 2-DOF PID regulator is designed by modifying (3.23) in form of equation (3.24), and Figure 8 shows the block diagram of this algorithm.

$$u(s) = K_p[(b \cdot r - y) + \frac{K_i}{s}e_i + \frac{s}{K_d + s/N}e) \quad \textbf{(3.24)}$$

Furthermore, an anti-windup scheme is implemented into I-regulator that its input e_i is re-shaped by back calculation and tracking algorithm

$$e_i = \begin{cases} e, & |u_0| < u_{sat} \\ e - K_t e_u, & |u_0| \geq u_{sat} \end{cases} \quad (3.25)$$

Figure 8. DOF PID regulator with back calculation and tracking algorithm

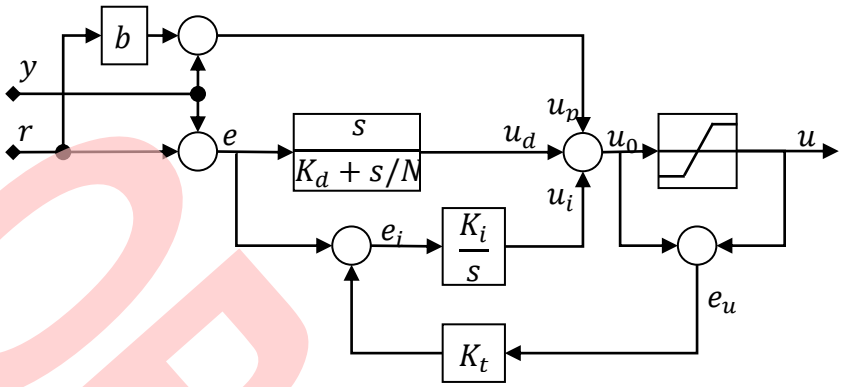

In this PID regulator, the tuning parameters goes up to 5 with the limitation that

$0 < b \leq 1$,

$K_i \leq K_t \leq K_d$, and $K_t = \sqrt{K_i K_d}$ is recommended for stability reason,

N is a large number of the order of 100 for filtering the input of D-regulator.

3.2.2 Sliding Mode Rotor Flux Observer

Considering induction motor model in $\alpha\beta$ reference frame, equations (3.1)~(3.8) is simplified by eliminating $\lambda_{\alpha s}$,$\lambda_{\beta s}$, $i_{\alpha r}$, and $i_{\beta r}$, therefore motor model is reassembled as

$$V_{\alpha s} = \left(R_s + \frac{{L_M}^2}{{L_r}^2} R_r\right) i_{\alpha s} + \frac{L_s L_r - {L_M}^2}{L_r} \frac{d}{dt} i_{\alpha s} - \frac{L_M R_r}{{L_r}^2} \lambda_{\alpha r} - \omega_r \frac{L_M}{L_r} \lambda_{\beta r} \quad \textbf{(3.26)}$$

$$V_{\beta s} = \left(R_s + \frac{{L_M}^2}{{L_r}^2} R_r\right) i_{\beta s} + \frac{L_s L_r - {L_M}^2}{L_r} \frac{d}{dt} i_{\beta s} - \frac{L_M R_r}{{L_r}^2} \lambda_{\beta r} + \omega_r \frac{L_M}{L_r} \lambda_{\alpha r} \quad \textbf{(3.27)}$$

$$\frac{d}{dt} \lambda_{\alpha r} = -\frac{R_r}{L_r} \lambda_{\alpha r} + \frac{R_r L_M}{L_r} i_{\alpha s} - \omega_r \lambda_{\beta r} \quad \textbf{(3.28)}$$

$$\frac{d}{dt} \lambda_{\beta r} = -\frac{R_r}{L_r} \lambda_{\beta r} + \frac{R_r L_M}{L_r} i_{\beta s} + \omega_r \lambda_{\alpha r} \quad \textbf{(3.29)}$$

Let $x = [i_{\alpha s}, i_{\beta s}, \lambda_{\alpha r}, \lambda_{\beta r}]^T$ be the states of system, induction motor model expressed in state-space form is

$$\frac{d}{dt} x = Ax + Bu_s \quad \textbf{(3.30)}$$

where

$u_s = \begin{bmatrix} V_{\alpha s} \\ V_{\beta s} \\ 0 \\ 0 \end{bmatrix}$ is the input stator voltage vector.

$$A = \begin{bmatrix} -\frac{R_{eq}}{\sigma L_s} & 0 & \frac{k_r}{\sigma L_s \tau_r} & \frac{\omega_r k_r}{\sigma L_s} \\ 0 & -\frac{R_{eq}}{\sigma L_s} & -\frac{\omega_r k_r}{\sigma L_s} & \frac{k_r}{\sigma L_s \tau_r} \\ \frac{L_M}{\tau_r} & 0 & -\frac{1}{\tau_r} & -\omega_r \\ 0 & \frac{L_M}{\tau_r} & \omega_r & -\frac{1}{\tau_r} \end{bmatrix}, B = \begin{bmatrix} \frac{1}{\sigma L_s} & 0 \\ 0 & \frac{1}{\sigma L_s} \\ 0 & 0 \\ 0 & 0 \end{bmatrix}$$

Now, let $\hat{x} = [\hat{\imath}_{\alpha s}, \hat{\imath}_{\beta s}, \hat{\lambda}_{\alpha r}, \hat{\lambda}_{\beta r}]^T$ be the estimated states, and a sliding mode observer is designed as

$$\frac{d}{dt}\hat{x} = A\hat{x} + Bu + Kv \quad \textbf{(3.31)}$$

where

$$K = \begin{bmatrix} k & 0 & 0 & 0 \\ 0 & k & 0 & 0 \\ 0 & 0 & 0 & 0 \\ 0 & 0 & 0 & 0 \end{bmatrix}, \text{ and } v = \begin{bmatrix} sign(i_{\alpha s} - \hat{i}_{\alpha s}) \\ sign(i_{\beta s} - \hat{i}_{\beta s}) \\ 0 \\ 0 \end{bmatrix}$$

It is not difficult to demonstrate that the output of observer ($\hat{x}$) converges to x when k is a relative large positive constant. Figure 9 shows the block diagram of the designed sliding mode observer, and the rotor flux angle is calculated by estimated flux vector

$$\theta_\Psi = \arctan\left(\frac{\hat{\lambda}_{\beta r}}{\hat{\lambda}_{\alpha r}}\right) \quad \textbf{(3.32)}$$

Figure 9. Block diagram of sliding mode rotor flux observer

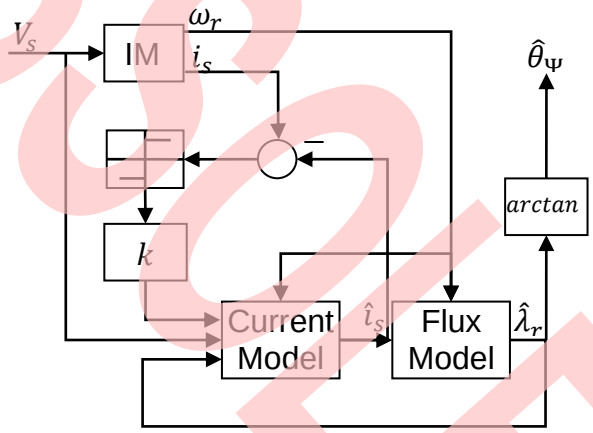

3.2.3 Dead Time Compensation

To avoid the shoot-through of DC link, a short period named dead time is enforced in the SVPWM scheme, and thus a load dependent voltage distortion causes the mismatch between command voltage and actual voltage. Besides this dead time, the voltage loss on thyristors and diodes also result in voltage error, and the output voltage mismatch due to the adversity of these three factors is called “dead time effect”.

Figure 10 shows a typical connection of three-phase inverter. Taking the bridge of a-phase as an example, the magnitude of V_a in a switch period is analysed in Figure 11, in which t_d is dead time, t_{on} is the delay time when switch on thyristor, t_{off} is the delay time when switch off thyristor, V_s is voltage loss on thyristor, V_d is voltage loss on diode, V_{dc} is DC voltage, t is ideal conduction time, and T is SVPWM period. Hence, the actual voltage can be calculated by average theory as

$$V_a = \begin{cases} V_{ideal} - \frac{t_d + t_{on} - t_{off}}{T} V_{dc} - \frac{T - t + t_d + t_{on} - t_{off}}{T} V_s - \frac{t - t_d - t_{on} + t_{off}}{T} V_d, & i_a > 0 \\ V_{ideal} - \frac{t_d + t_{on} - t_{off}}{T} V_{dc} + \frac{T - t + t_d + t_{on} - t_{off}}{T} V_s + \frac{t - t_d - t_{on} + t_{off}}{T} V_d, & i_a < 0 \end{cases} \quad \textbf{(3.33)}$$

Figure 10. Typical three-phase inverter schematic

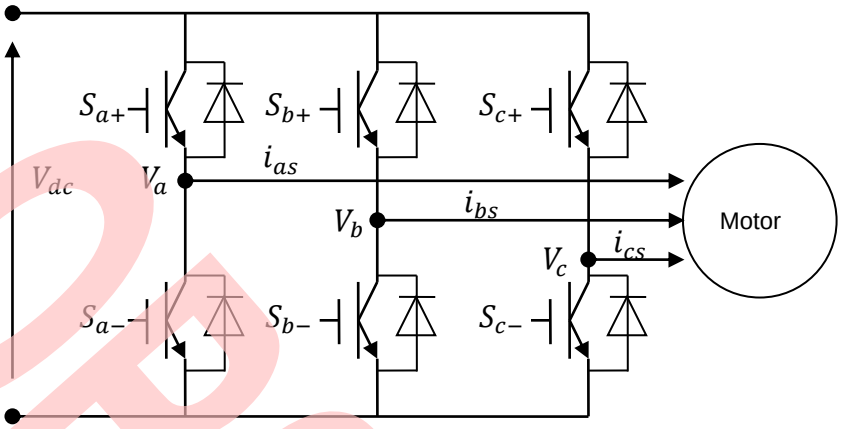

Figure 11. Dead time effect on output voltage

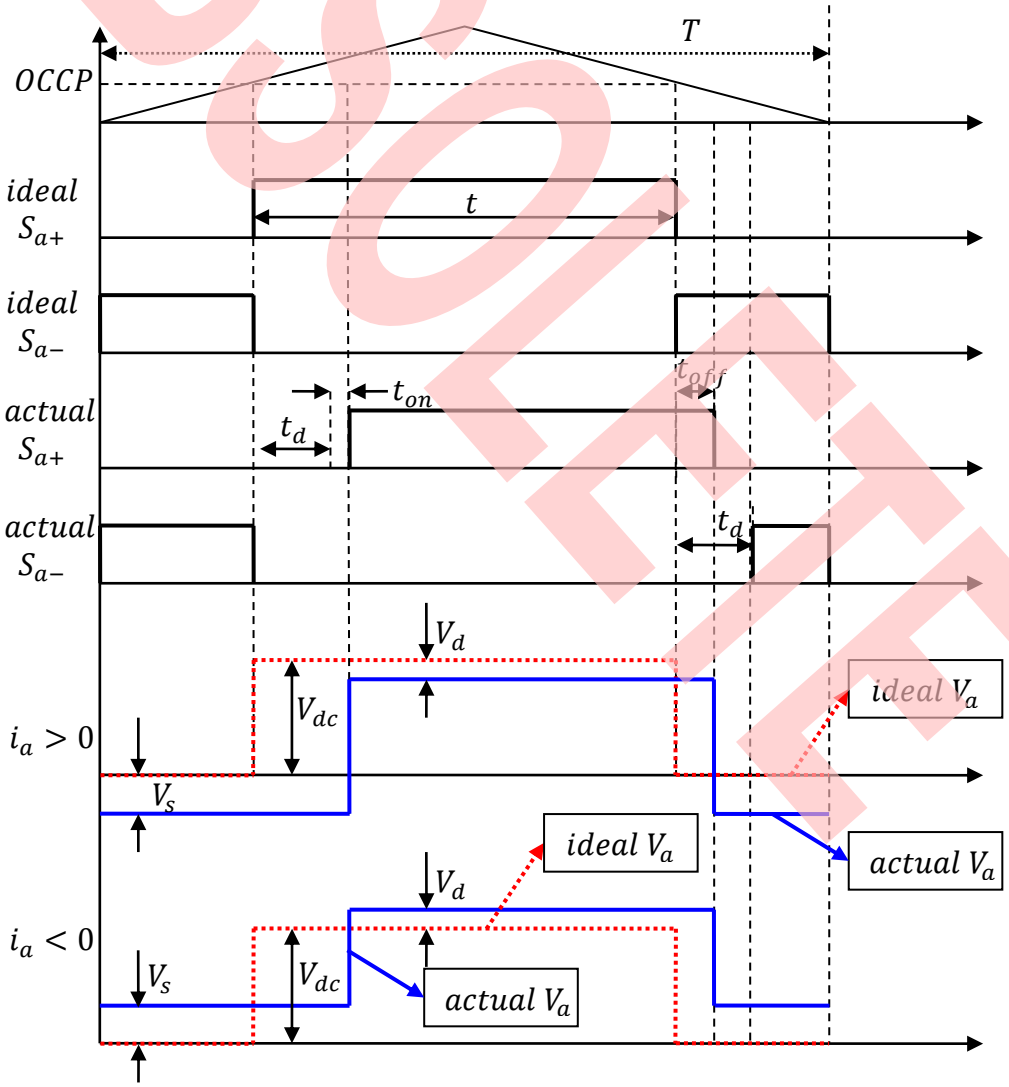

And the compensation voltage thus is defined as (3.34)

$$V_{com} = \begin{cases} -\frac{t_d+t_{on}-t_{off}}{T}V_{dc} - \frac{T-t+t_d+t_{on}-t_{off}}{T}V_s - \frac{t-t_d-t_{on}+t_{off}}{T}V_d, & i_a > 0 \\ -\frac{t_d+t_{on}-t_{off}}{T}V_{dc} + \frac{T-t+t_d+t_{on}-t_{off}}{T}V_s + \frac{t-t_d-t_{on}+t_{off}}{T}V_d, & i_a < 0 \end{cases} \quad \textbf{(3.34)}$$

Equation (3.34) shows that voltage loss in abc reference frame relates to current direction, which means current direction is a criterion of feeding compensation voltage. Particularly, when the current is crossing zero, voltage loss becomes ambiguity. Thus, solutions are made such that rotating current is usually used to judge compensation scheme. In this document, current vector in $\alpha\beta$ reference frame is utilized to calculate compensation voltage.

3.2.4 Field Weakening Control

As the motor runs at higher speed, back-EMF will occupy a large proportion of feeding voltage and thus rotor speed is limited since voltage is not tuneable. Field weakening control is a suitable solution that operates motor in constant power region and enlarges speed operation region.

Consider steady state of induction motor model (3.9)~(3.16), and assume rotor field oriented control is achieved, stator voltage model thus is written as

$$V_{ds} = R_s i_{ds} - \omega\sigma L_s i_{qs} \quad \textbf{(3.35)}$$

$$V_{qs} = R_s i_{qs} + \omega L_s i_{ds} \quad \textbf{(3.36)}$$

Ignore voltage drop on resistance, voltage V_{ds} and V_{qs} are limited due to inverter capability that

$$V_{ds}^2 + V_{qs}^2 = (\omega\sigma L_s i_{qs})^2 + (\omega\sigma L_s i_{qs})^2 \le \frac{V_{DC}^2}{3} \quad \textbf{(3.37)}$$

In another hand, the maximum current capability of motor is also a limitation of operation, and is expressed as

$$i_{ds}^2 + i_{qs}^2 \le i_{smax}^2 \quad \textbf{(3.38)}$$

Equation (3.37) and (3.38) indicates the actual available operation region due to voltage and current limitation, and Figure 12 plots the limitation curves as function of current, where the ellipses (dash lines) are voltage limitation curve, the cycle (red, solid line) is current limitation curve, and the hyperbola (blue, solid line) are equal-torque curves.

Figure 12. Voltage and current limitation curves

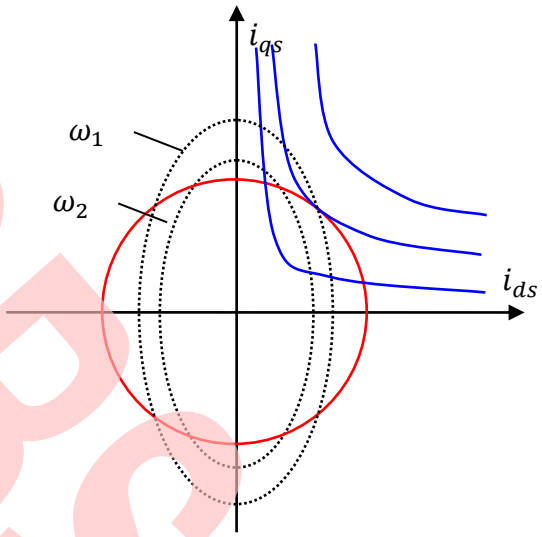

In this firmware, a gradient method is applied to generate reference d-axis current i_{ds}. Investigating voltage equation (3.35) and (3.36), and define a cost function as

$$J = \frac{1}{2}(V_{ds} - V_{dlim})^2 + \frac{1}{2}(V_{qs} - V_{qlim})^2 \quad \textbf{(3.39)}$$

Therefore, a control target is set to minimize the cost function. Taking partial difference to equation (3.39)

$$\frac{\partial J}{\partial i_{ds}} = \omega L_s(V_{qs} - V_{qlim}) \quad \textbf{(3.40)}$$

$$\frac{\partial J}{\partial i_{qs}} = -\sigma\omega L_s(V_{ds} - V_{dlim}) \quad \textbf{(3.41)}$$

Then the gradient method can be designed in digital form that

$$i_{ds}^*(n) = i_{ds}^*(n-1) - k * \frac{\partial J}{\partial i_{ds}} = i_{ds}^*(n-1) - k\omega L_s(V_{qs} - V_{qlim}) \quad \textbf{(3.42)}$$

where k is the gradient gain of flux controller.

4 Experiment Result

4.1 Parameter Measurement

Table 1. Parameter measurement result

Motor Parameter		Spec. Value	Measured Value	Unit	Error
Stator Resistance	R_s	1.6173	1.6076	Ω	0.6%
Rotor Resistance	R_r	1.6477	2.7116	Ω	64.6%
Mutual Inductance	L_m	170.7246	128.63	mH	24.7%
Stator Leakage Inductance	L_{ls}	6.7255	13.47	mH	100.1%
Rotor Leakage Inductance	L_{lr}	9.0637	13.47	mH	48.6%

4.2 Sensor-FOC Drive Performance

Figure 13. Experiment Platform

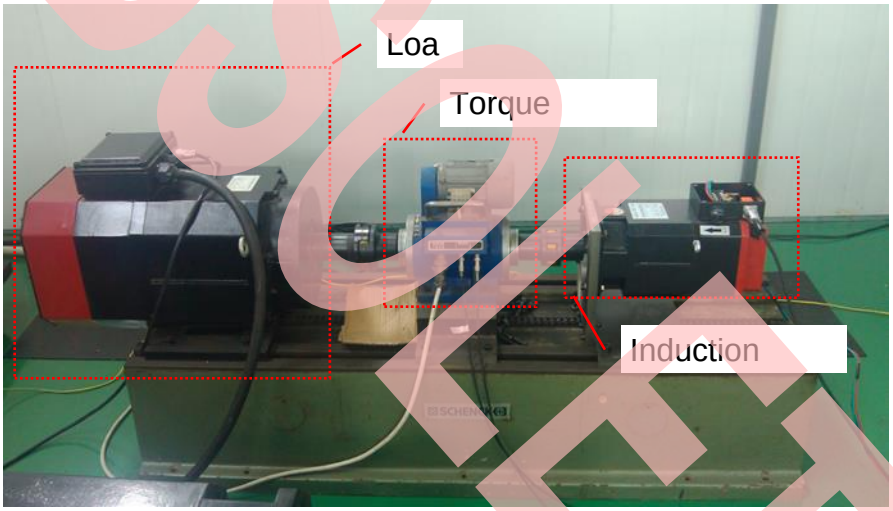

Figure 13 shows the configuration of experiment platform. The PMSM is controlled by a converter in tracking reference torque mode. The torque sensor is installed between load and testing motor thus the output torque of induction motor is measurement.

The experiment motor has parameters as table 1 shows.

Figure 14. FOC drive performance (T_l=0)

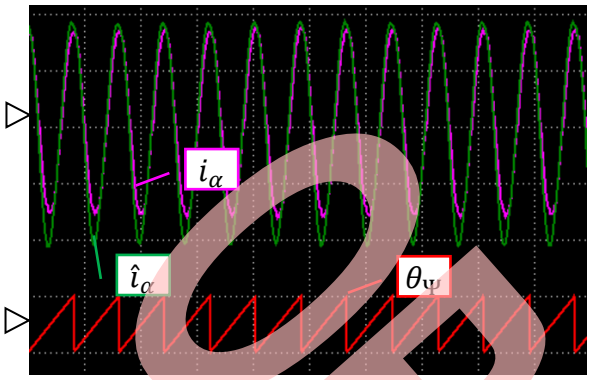

c). Estimated current (2A/div) and flux angle @30Hz

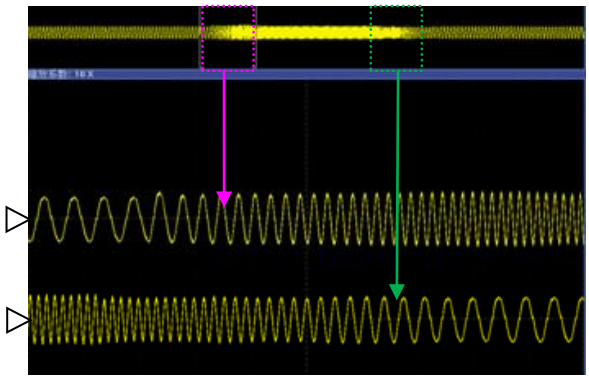

d). Motor phase current at acceleration and deceleration (2A/div)

Figure 15. FOC drive performance (T_l≠0)

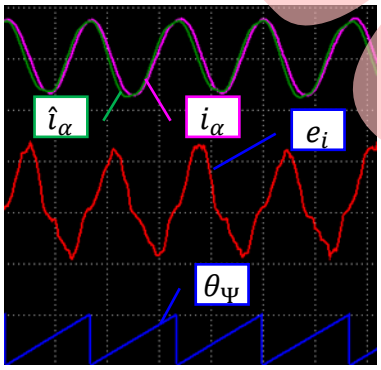

a). Estimated current (5A/div) current error (1A/div), and flux angle @30 Hz

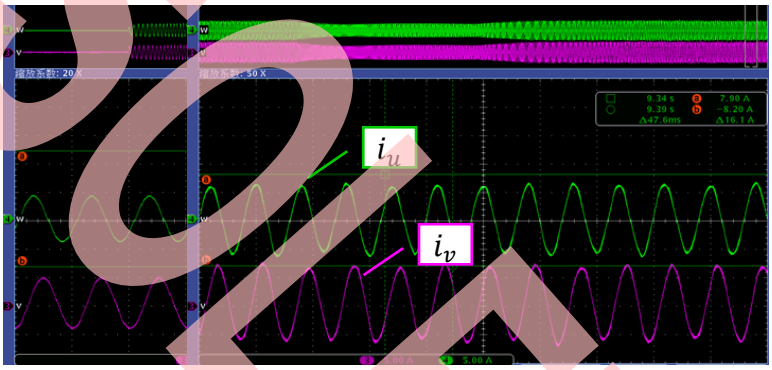

b). Stator current at startup, decrease load, and increase load @30 Hz

Figure 16 shows the field weakening performance of the induction motor. In this experiment, the DC voltage is set to 110 volt, and the reference speed is set 50Hz with/without field weakening operation. From picture (a), it can be seen that with rated magnetizing current, the maximum speed is about 20Hz and (b) shows stator current in this case.

Picture (c), (d), (e), and (f) show the field weakening performance, and the maximum speed goes up to 45Hz. Picture (c) shows the magnetizing current and speed response when motor switches operation mode from normal region to field weakening region, and picture (d) shows stator current response in this procedure.

Picture (e) shows the same state when motor switches operation mode from field weakening region to normal region, and picture (f) shows stator current response in this procedure.

Figure 16. Motor response with/without field weakening

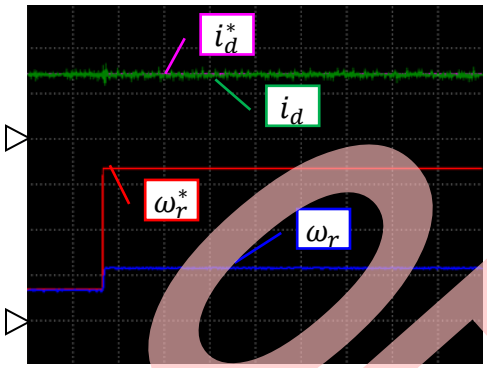

a). Magnetizing current (2A/div) and speed (15Hz/div)response without field weakening

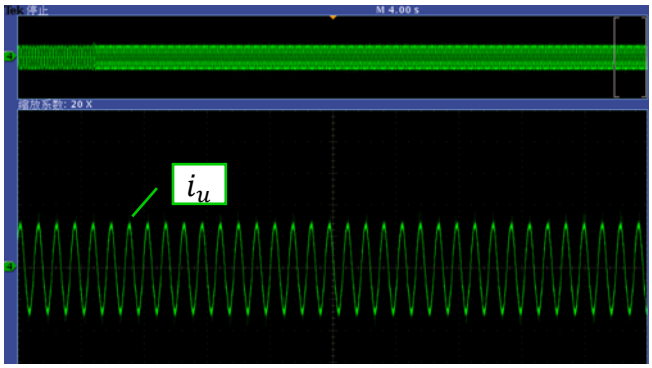

b). Stator current (2A/div) without field weakening

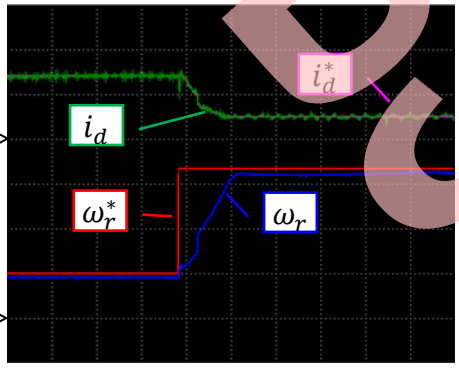

c). Magnetizing current (2A/div) and speed (15Hz/div) response with field weakening

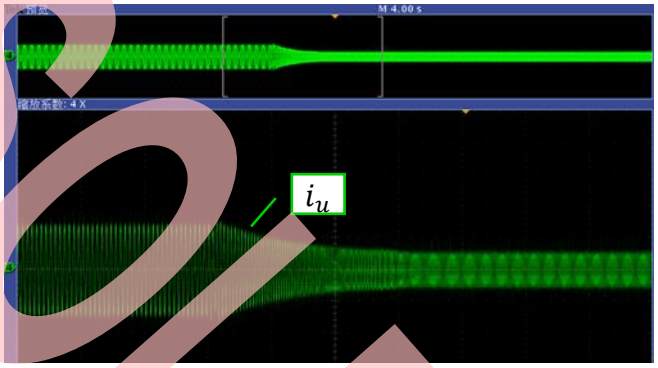

d). Stator current (2A/div) with field weakening

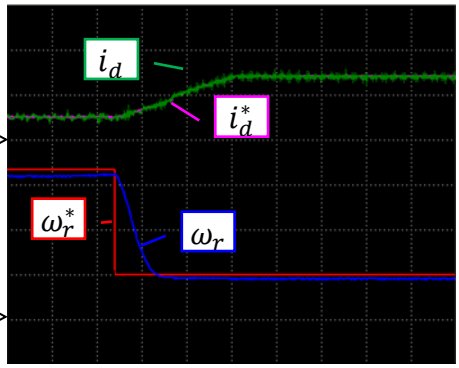

e). Magnetizing current (2A/div) and speed (15Hz/div) response with field weakening

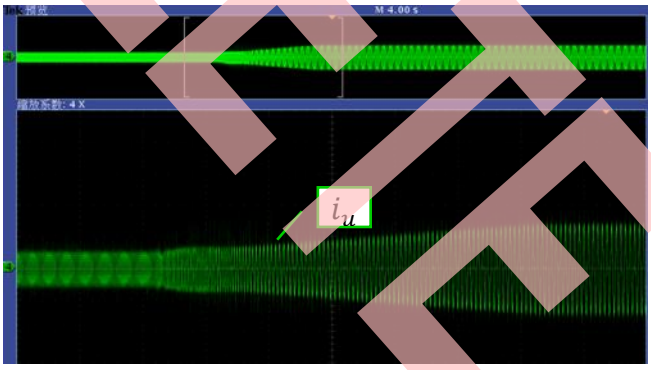

f). Stator current (2A/div) with field weakening

5 Document History

Document Title: AN205408 - SMO Based Field Oriented Control of Induction Motor with Speed Sensor

Document Number: 002-05408

Revision	ECN	Orig. of Change	Submission Date	Description of Change
**	_	XINL	31/08/2012	1.0.0 First Draft
			12/09/2012	1.1.0
			09/10/2012	1.2.0 Add Field weakening
*A	5041849	XINL	12/28/2015	Converted Spansion Application Note “MCU-AN-510124-E-12” to Cypress format
*B	5840864	AESATMP9	08/03/2017	Updated logo and copyright.
*C	6329249	SSAS	10/02/2018	Obsoleted

Worldwide Sales and Design Support

Cypress maintains a worldwide network of offices, solution centers, manufacturer's representatives, and distributors. To find the office closest to you, visit us at Cypress Locations.

Products

ARM® Cortex® Microcontrollers	cypress.com/arm
Automotive	cypress.com/automotive
Clocks & Buffers	cypress.com/clocks
Interface	cypress.com/interface
Internet of Things	cypress.com/iot
Memory	cypress.com/memory
Microcontrollers	cypress.com/mcu
PSoC	cypress.com/psoc
Power Management ICs	cypress.com/pmic
Touch Sensing	cypress.com/touch
USB Controllers	cypress.com/usb
Wireless Connectivity	cypress.com/wireless

PSoC® Solutions

PSoC 1 | PSoC 3 | PSoC 4 | PSoC 5LP | PSoC 6

Cypress Developer Community

Forums | WICED IOT Forums | Projects | Videos | Blogs | Training | Components

Technical Support

cypress.com/support

Cypress Semiconductor
198 Champion Court
San Jose, CA 95134-1709